# Modification of limestone alkali-activation by addition of grinded glass

**Annelise COUSTURE[1], Norbert RENAULT[1], Khadim NDIAYE[1], Jean-Louis GALLIAS[1]**

[1] *L2MGC, CY Cergy Paris Université, 95000 Cergy Pontoise*

**ABSTRACT** The development of alkali-activated materials for construction has grown over the past 20 years due to the reduction of environmental impact compared to cementitious materials. In case of materials with high calcium content (limestone) activated by soda solution (without silicate), it is possible, with an optimized formulation, to obtain mortars with compressive strength of 20MPa. The activation products are pirssonite and portlandite. However, due to their solubility, these materials lose much of their mechanical strength in high humidity environments. In order to resolve this problem, finely grinded glass, from recycling bottles, was added at different amounts. The impact of this addition was studied in terms of reaction process, fresh and hardened properties. The addition of grinded glass led to formation of new products, probably hydrated, which are responsible of a significant reduction of mortar porosity but the compressive strength, at 28 days, decreased overall 23% compared to mortars without grinded glass. However, the behavior in humidity environments was significantly improved and the compressive strength was maintained after a leaching test.

**Keywords** alkali-activation, limestone, grinded glass, leaching

## I.  INTRODUCTION

Binders based on alkaline activation of raw materials (containing mainly silica and alumina) is a subject of increasing importance for construction during at least the last 20 years. These materials have a lower environmental impact than cementitious materials [1, 2]. Alkali-activation of raw material with high calcium content (limestone) by soda solution (without silicate) was barely studied [3-5] even if its environmental impact is also very low [4]. Their alkali-activation produces alkali-carbonate crystallized phases (gaylussite and/or pirssonite and/or thermonatrite) and/or portlandite. With an appropriate optimization of formulations and curing parameters, they can reach a compressive strength of 20MPa [5]. However, due to solubility of reaction products, these binders are not appropriate for use in humidity environments. A solution to solve this problem is to generate insoluble hydrated phases such as silica gels and/or x-S-H phases (with x= C or N or N-C). It is therefore necessary to incorporate active siliceous compounds. They can be added in the activator solution (for example, sodium silicate solution but the cost increases significantly) [4] or as a co-precursor (waste glass from recycling) [3]. Waste glass is an interesting raw material because its use in construction materials can reduce environmental pollution, save building material resources [6] and is efficient precursor in alkaline activation [7, 8]. This study focuses on the influence of glass addition on alkaline activation of limestone with sodium hydroxide. Firstly, the kinetics reaction was followed and the products of the reaction, regarding the glass amount,

were identified. Moreover, the properties of the mortars on fresh and hardened states were determinated. Finally, the behavior of optimized formulation without and with glass, in water environment, was assessed after a homemade leaching test.

## II.  MATERIALS AND METHODS

### A.  *Precursors and alkaline activator*

The limestone (LS) was a pure limestone filler commonly used as an addition in concrete. Calcite was the only crystallized mineral identified by XRD. The grinded glass (GG) comes from the recycling of colored green glass bottles (cleaned, crushed and grinded 1 min at 1000 rotation per minute in a vibratory disc mill). Only the granular fraction lower than 100µm was kept after a sieving [7]. Table 1 summarized physical and chemical characteristics of the two precursors.

TABLE 1.   **Physicals properties and chemical analysis of LS (from supplier) and GG (measured)**

| | **Physical properties** | | | **Chemical analysis (%)** | |
|---|---|---|---|---|---|
| LS | Absolute density (kg/m³) | 2700 | | $CaCO_3$ | 98.3 |
| | Specific area (m²/kg) (*BET*) | 2914 | | $SiO_2$ | 0.1 |
| | Particles size < 63 µm (%) | 97 | | $Na_2O$ | 0.01 |
| GG | Specific area (m²/kg) (*BET*) | 650 | | $SiO_2$ | 70.7 |
| | Particle distribution (µm) | dv10 | 3.23 | $Na_2O$ | 13.8 |
| | | dv50 | 11.5 | CaO | 11.6 |
| | | dv90 | 34.9 | Other oxides | 3.9 |

The activator used in this study was a solution of sodium hydroxide (NaOH) at 13 mol/L obtained by dilution of concentrated soda solution 50 %wt (i.e. 19 mol/L). The pH was around 15.

### B.  *Mortar preparation and curing*

All materials were held in climatic chamber at 20°C at least for 24 hours before mixing. Mortars were made of one part of LS and three parts of standardized sand with a water to reagent ratio (W/R) equal to 0.45 (optimized formulation [5]). W was the mass of water (including water from NaOH solution) and R was the mass of reagents from LS ($CaCO_3$), GG ($SiO_2$, $Na_2O$ and CaO) and soda solution ($Na_2O$). Moreover, a $SiO_{2(GG)}/Na_2O$ ratio was determinated. All the tested compositions were presented in Table 2.

TABLE 2.   **Compositions of mortars**

| | **Theorical quantities (%wt)** | | | | | | | |
|---|---|---|---|---|---|---|---|---|
| **$SiO_{2(GG)}/Na_2O$** | **$SiO_2$ (sand)** | **$CaCO_3$ (LS)** | **$SiO_2$ (GG)** | **Impurities (sand, LS and GG)** | **$Na_2O$ (solution+ GG)** | **CaO (GG)** | **$H_2O$** | **Total** |
| 0 | 60.05 | 20.45 | 0.00 | 2.73 | 4.96 | 0.00 | 11.81 | 100.00 |
| 0.35 | 56.85 | 19.36 | 2.09 | 2.70 | 5.94 | 0.34 | 12.72 | 100.00 |
| 0.62 | 54.32 | 18.50 | 3.99 | 2.69 | 6.42 | 0.66 | 13.42 | 100.00 |
| 0.82 | 51.82 | 17.65 | 5.78 | 2.67 | 7.06 | 0.95 | 14.07 | 100.00 |

The mortars were mixed according to standard EN NF 196-1 [9] and three 40x40x160mm prismatic specimens were cast in two layers, vibrated for 30s each, to release residual air bubbles. The molds were sealed in plastic bags until demolding (3 days). The specimens continue their curing in sealed plastic bags (11 days) and are dried at 45°C (14 days) in order to eliminate free water, responsible of internal stresses [4].

*C. Test methods*

Kinetics of alkali-activation was characterized on pastes, by semi-adiabatic calorimetry experiments (room at 20±0.2°C). The heat evolved was determined as in the standard NF EN 196-9 [10] but specific heat capacity of cement and sand were replaced by those of calcite, sodium oxide and glass (0,815 ; 1,114 and 0,7937 J/K/g, respectively [11-13]). The paste was directly hand-mixed during 1min 35s after soda solution introduction into the steel vessel. The mortars have been tested in fresh and hardened states: the workability was assessed by mini-cone slump test (EN NF 12350-2 relative to Abram's cone [14]). The flexural and compressive strengths of the cured specimens (i.e. 28 days) were measured (NF EN 196-1 [9]), using 3R Quantech apparatus with loading speeds of 50 and 2400N/s for flexural and compressive strength tests, respectively. Porosity measurements (EN NF 1936 [15] and NF P18-459 [16]) were made, at 32 days, using absolute ethanol instead of water in order to avoid the possible dissolution of alkali-activation products. Moreover, others characterizations were performed: the weight loss of the specimens, expressed as a percentage of the initial mass, was monitored throughout the curing time (28 days) by weighing once a day. Thermal analysis (at 32-35 days) and FTIR (at 35 days) spectra were carried out, on representative samples of 3 prismatic specimens, used for mechanical test, after grinding (less than 0.315mm) and homogenization of 50g of mortar into powder, which were then sealed in plastics bags until testing. DTA-TGA tests were performed with a STA 449 F1 Jupiter analyzer (Netzsch), on 110mg of powder, from 25°C to 1000°C (heating rate of 10°C/min) under dynamic nitrogen atmosphere. FTIR spectra were recorded, in the range of 4000–600 cm$^{-1}$, with an Alpha spectrometer (Bruker). The microstructure was observed by scanning electron microscopy (Gemini 300, ZEISS) on platinum-coated fractured pieces of cured specimens at 10kV. A leaching test was proposed and performed on optimized mortar (lowest porosity and highest compressive strength) with and without GG: it consists in immersion of the dried specimens in tap water for 28 days (weight ratio of water to specimen equal to 2) followed by a drying at 45°C for 14 days. During this test, the weight and the dimension of the specimens were measured as well as the pH of the water. At the end of this test, the mechanical strengths were measured again.

## III.   RESULTS AND DISCUSSION

*A. Kinetics modification*

Calorimetric curve for the alkali-activated paste with $SiO_{2(GG)}/Na_2O$ = 0 and 0.62 are presented in Figure 1: Fig. 1a) shows the heat evolution for the first 14 days (corresponding to storage time of specimens in sealed plastic bags) and Fig 1b) describe the heat evolution for the first hour. Immediately after the beginning of recording, the heat sharply increases until it reaches 36.3 and 25.1 J/g in approximately 8 and 15 minutes for pastes with $SiO_{2(GG)}/Na_2O$ = 0 and 0.62, respectively.
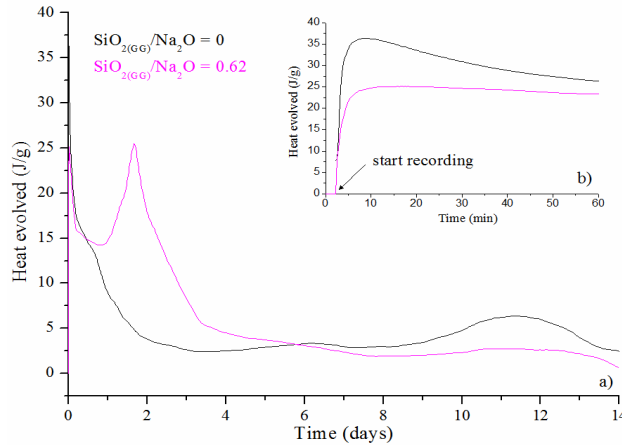
**FIGURE 1.** Heat of hydration of alkali-activated pastes with $SiO_{2(GG)}/Na_2O = 0$ and $0.62$

The addition of GG slows down the rate and the heat evolved of the limestone dissolution in contact with soda solution (first exothermic phase). After 5 hours, the gradual decrease in heat (related to structuration of pirssonite in paste without GG) changes with the addition of GG: another peak was observed between 1 and 3 days with a maximum at around 1.5 day (24.6 J/g). This indicates a new reaction and the formation of a new product. At the end of the test (14 days), the heat reaches a minimum at around 2.5 and 0.6 J/g for pastes with a $SiO_{2(GG)}/Na_2O = 0$ and 0.62, respectively. It therefore seems that the reaction process is finished at 14 days. The kinetic was also followed by monitoring the weight loss of specimen's mortars during their curing (Figure 2).
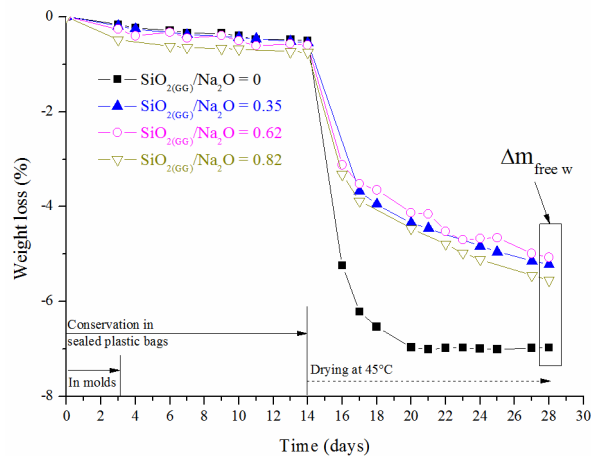


**FIGURE 2.** Average weight loss of alkali-activated mortars during their curing

For all formulations, the standard deviation for weight loss between the different specimens was very low (less than 0.31%). This indicate the great homogeneity of the mortars. During conservation in plastic bags for 14 days, weight loss was low (around 0.75% of the initial mass). It was followed by a great loss of weight during the first days of drying at 45°C. When GG was added ($SiO_{2(GG)}/Na_2O \geq 0.35$), the weight loss became less pronounced without reaching a stabilized value ($\Delta m_{free\ w}$) at the end of drying. So, the evaporation kinetics was slow down and the

introduction of GG leads to an additional consumption of water during the curing and confirms the formation of new reaction product.

## B. Identification of reaction products

The average curves of each composition with and without GG are presented in Figure 3. For all formulations, dissociation reactions (peaks with mass loss, ① to ⑤) and crystallographic transformations (peaks without mass variation ❶ and ❷) were identified.
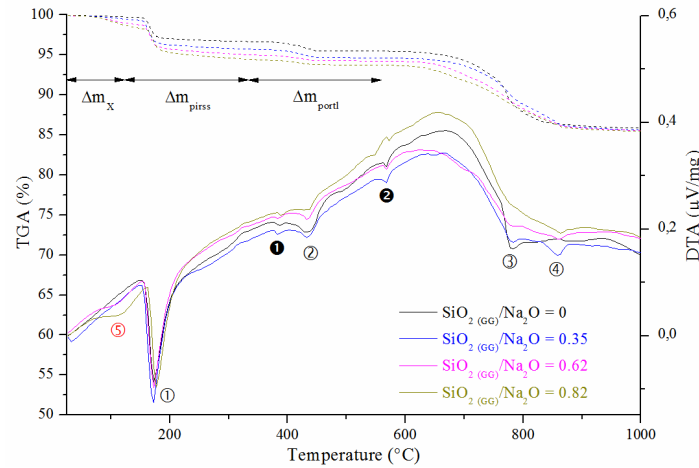


**FIGURE 3.**    **TGA (dash) and DTA (solid) average curves of mortars samples (all formulations) after 28 days curing**

The peaks ① to ④ (at 175, 435, 775 and above 800°C) were related to dehydration of pirssonite, portlandite, decarbonatation of nyerereite (resulting from dehydration of pirssonite) and calcite, respectively. The crystallographic transformations (at 386°C and 567°C) were related to transition of nyerereite from low to high temperature and to allotropic transformation of quartz $\alpha$ into quartz $\beta$, respectively. All the temperatures were consistent with the literature [17, 18]. When the $SiO_{2(GG)}/Na_2O$ ratio increase a new dissociation peak (⑤ at 110°C) appears and become more and more visible. It confirms the formation of a new reaction product most probably hydrated. The weight loss of reaction products were measured on TGA curves then bound water ($\Delta m_{bound\ w}$) and total water ($\Delta m_{water}$) were calculated by a methodology previously proposed [5]. The results are gathering in Table 3.

**TABLE 3.**    **Water composition of mortars after alkali-activation**

| $SiO_{2(GG)}/Na_2O$ | | 0 | 0.35 | 0.62 | 0.82 |
|---|---|---|---|---|---|
| Weight loss (%) TGA curves | New product ($\Delta m_{X(TGA)}$, 75-125°C) | 0.00 | 0.34 | 0.74 | 1.05 |
| | Pirssonite ($\Delta m_{pirss(TGA)}$, 125-335°C) | 3.28 | 3.77 | 3.95 | 4.14 |
| | Portlandite ($\Delta m_{portl(TGA)}$, 335-560°C) | 1.20 | 1.10 | 0.79 | 0.73 |
| Free water $\Delta m_{free\ w}$ (%) | | 6.97 | 5.21 | 5.07 | 5.55 |
| Bound water $\Delta m_{bound\ w}$ (%) | New product ($\Delta m_{X\ w}$) | 0.00 | 0.32 | 0.70 | 0.99 |
| | Pirssonite ($\Delta m_{pirss\ w}$) | 3.05 | 3.57 | 3.75 | 3.91 |
| | Portlandite ($\Delta m_{portl\ w}$) | 1.12 | 1.04 | 0.75 | 0.69 |
| Total water $\Delta m_{water}$ (%) | | 11.42 | 10.15 | 10.27 | 11.14 |

The bound water loss of the new product and pirssonite increases when the $SiO_{2(GG)}/Na_2O$ ratio increases. It goes along with a decrease of the bound water in portlandite. This indicates the participation of portlandite in the formation of the new hydrate. When the water in mortars, after alkali-activation, is compared to initial water (Table 2), the difference was very low (0.67%) for mortars without GG but increase for mortars with GG (around 3%). This could be due to incomplete reaction in the alkali-activated process, especially during the drying (already seen in Fig. 2). Example of microstructure of mortar with GG was presented in Figure 4.
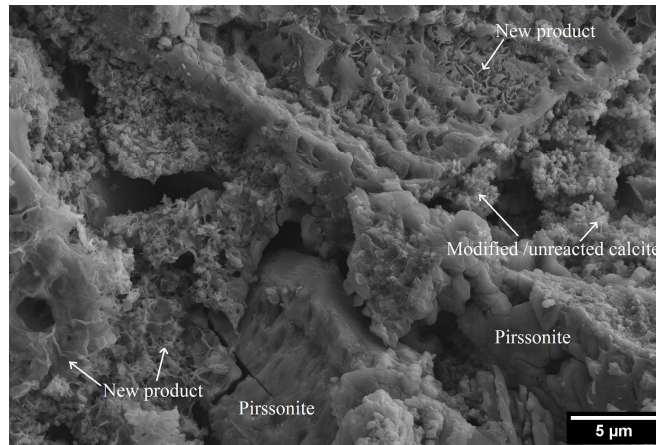


**FIGURE 4.**     **SEM images of mortar pastes with $SiO_{2(GG)}/Na_2O = 0\ 62$**

The paste of mortar changes when GG is added: as well as dense (pirssonite) and grainy areas (modified and/or unreacted calcite) [5] a new microstructure was observed. Its fluffy and thin-skinned structure is close to the honeycomb microstructure of the alkali-silica reaction (ASR) products [19]. The identification of this new product was carried out by FTIR spectra and the results were presented in Figure 5. The FTIR spectrum of sample without GG presents characteristics peaks of sand (1162, 1091, 796, 778 cm$^{-1}$), pirssonite (1484-1411, 1068, 695 and 660 cm$^{-1}$), portlandite (3644 cm$^{-1}$), calcite (872 and 711 cm$^{-1}$) and water (broadband between 3500-3000 cm$^{-1}$). There were consistent with the literature [20-22].
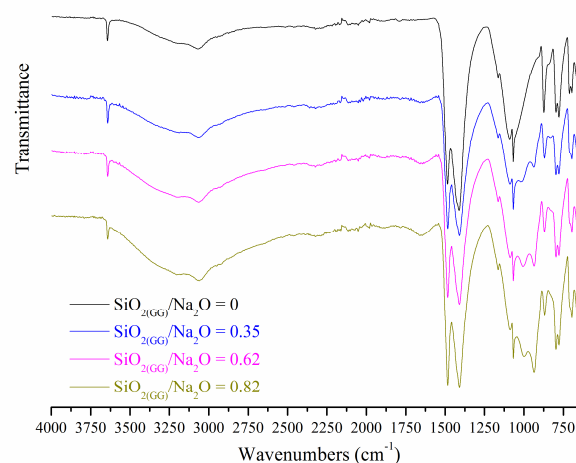


**FIGURE 5.**     **Average FTIR spectra of mortars samples (all formulations) after 28 days curing**

When GG is added, two new peaks appears at 1000 and 937 cm$^{-1}$. There were in the range corresponding to the asymmetric and symmetric stretching vibrations of Si–O bonds in silica gels incorporating $Ca^{2+}$ and $Al^{3+}$ cations/C-S-H structures [8, 23]. With the increase of GG, the broadband of water and the two new peaks increase while the portlandite peak decreases. This confirms the participation of portlandite (such as in ASR reaction) in the reaction process of the new product formation, which is hydrated and contain silicon oxide.

*C.  Modification of mortars properties (fresh and hardened state)*

Just after mixing, the workability was measured and improved from 0.21±0.07 to 0.28±0.03 to 0.78±0.17 and to 0.82±0.08cm for $SiO_{2(GG)}/Na_2O$ ratio of 0, 0.35, 0.62 and 0.82, respectively. It was explained by synergy of two phenomena: the increase of total water amount (Table 2) when GG is added in order to keep the W/R ratio constant and the slowing down in calcite dissolution (Fig. 1). Figure 6 gathers the mechanical strength and porosity obtained after curing: in one hand, the porosity was significantly reduced (until 50% for $SiO_{2(GG)}/Na_2O = 0.62$) when GG was added but was not linear. It was explained by the increase of pirssonite quantity (estimated by its bound water, Table 3) and by the presence of the new product.
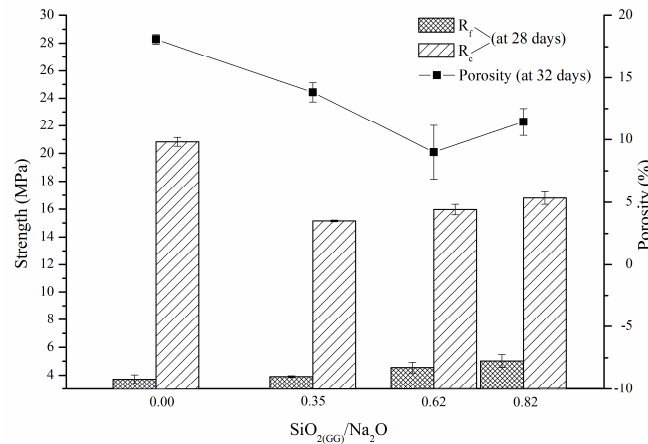


**FIGURE 6.**   **Mechanical strength and porosity of mortars with different $SiO_{2(GG)}/Na_2O$ ratio**

In the other hand, the flexural strength slightly increases with the $SiO_{2(GG)}/Na_2O$ ratio and the compressive strength decreases overall 23% when low amount of GG is added but with the increase in GG amount, which changes the products assemblies, the compressive strength slightly increases from 15.15 to 16.80MPa. The optimized formulation (lowest porosity and highest compressive strength) was obtained with a $SiO_{2(GG)}/Na_2O = 0.62$.

*D.  Leaching test*

Figure 7 presents the weight and the dimensional variation of optimized mortars, without and with GG, during the leaching test. Whatever the amount of GG, the pH of the water sharply increases during the first 5 days of specimen's immersion (from 8.3 to 13.5) and remain stable. After 3 days of immersion, the weight and the dimensional variations were similar for both formulations: an increase of weight (4%) and a swelling (0.03 and 0.05% with and without GG,

respectively) were observed due to the absorption of water. Once water saturation was reached, the weight gradually decrease (probably due to the dissolution of pirssonite) but the swelling still gradually increases.
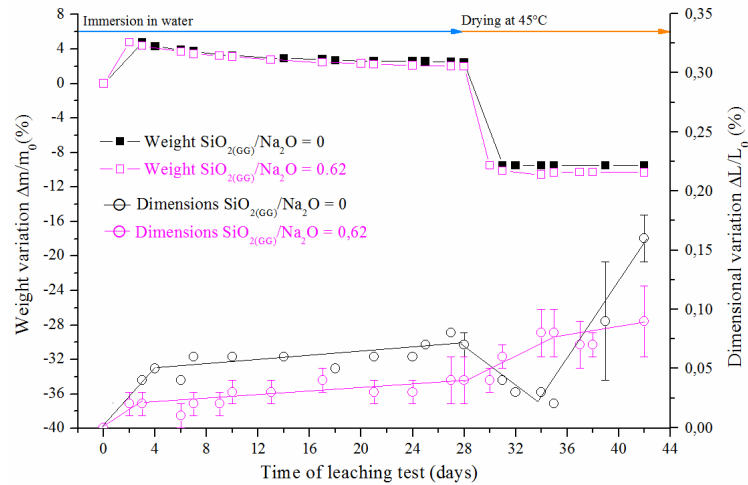


**FIGURE 7.** Average curves of weight and dimensional variations of mortars with $SiO_{2(GG)}/Na_2O = 0$ and 0.62 during the leaching test

During the first days of drying, the specimen's weight for both mortars, quickly decreases due to evaporation of residual adsorbed water but the dimensional variations differs. The specimens without GG presents a shrinkage (equivalent to the previous swelling) during 5-6 days of drying followed by a swelling until the end of the test while the specimens with GG gradually continues their swelling. However, at the end of the test, the swelling was lower for specimens with GG (<0.13 and 0.18% for mortar with $SiO_{2(GG)}/Na_2O$ ratio equal to 0.62 and 0, respectively). Table 4 gather the mechanical strengths before and after leaching test.

**TABLE 4.** Mechanical behavior of mortars ($SiO_{2(GG)}/Na_2O = 0$ and 0.62) before and after leaching test

| $SiO_{2(GG)}/Na_2O$ | At 28 days (before leaching test) | | At 70 days (after leaching test) | |
|---|---|---|---|---|
| | $R_f$ (MPa) | $R_c$ (MPa) | $R_f$ (MPa) | $R_c$ (MPa) |
| 0 | $3.71 \pm 0.32$ | $20.83 \pm 2.54$ | $1.68 \pm 0.16$ | Manual stop |
| 0.62 | $4.55 \pm 0.38$ | $15.97 \pm 0.47$ | $4.36 \pm 0.59$ | $16.62 \pm 1.28$ |

After leaching test, the mechanical behavior of specimens without GG was totally degraded: the flexural strength decreases about 55% and the compressive strength was no longer measurable. The specimens of optimized mortar with GG still have their strength. This result confirms that the addition of GG is a good solution to improve the behavior of alkali-activated mortars, with a high calcium content, in humidity environments.

## IV.   CONCLUSION

The aim of this study was to improve mechanical resistance of limestone alkali-activated mortars in high humidity environments by adding finely grinded glass from recycling bottles. The

investigation on kinetics reaction, fresh and hardened properties, characterization of reaction products, when GG was added, allows the following conclusions:

- The limestone dissolution by soda solution is slowing down but the global reaction process seems to be ended after 14 days.
- A new hydrated siliceous phase was generated (with the participation of portlandite) which seems to fill the porosity between the crystalline phases.
- The mechanical performances were reduced at 28 days but remain stable after the leaching test.

These results indicate that the proposed solution for improvement of limestone alkali-activated mortars, in high humidity environments, is a great and eco-friendly solution but further investigations, for example on time of drying, is needed to improve the mechanical behavior before leaching test.

## REFERENCES

[1] Shi, C., Krivenko, P.V., & Roy., D. (2006). Alkali-activated cements and concretes, *Taylor & Francis, Abingdon and New York*.

[2] Tang, Z., Li, W., Hu, Y., Zhou, J. L., & Tam, V. W. (2019). Review on designs and properties of multifunctional alkali-activated materials (AAMs), *Constr. Build. Mater.*, 200, 474-489. https://doi.org/10.1016/j.conbuildmat.2018.12.157

[3] Avila-Lopez, U., Almanza-Robles, J.M., & Escalente-Garcia, J.I. (2015). Investigation of a novel waste glass and limestone binders using statistical methods, *Constr. Build. Mater.*, 82, 296-303. https://doi.org/10.1016/j.conbuildmat.2015.02.085.

[4] Ortega-Zavala, D.E., Santana-Carrillo, J.L., Burciaga-Díaz, O., & Escalante-García, J.I. (2019). An initial study on alkali activated limestone binders, *Cem. Concr. Res.*, 120, 267–278. https://doi.org/10.1016/j.cemconres.2019.04.002.

[5] Cousture, A., Renault, N., Gallias, J-L., & Ndiaye, K. (2021). Study of a binder based on alkaline activated limestone, *Constr. Build. Mater.*, 311, 125323. https://doi.org/10.1016/j.conbuildmat.2021.125323.

[6] Guo, P., Meng, W., Nassif, H., Gou, H., & Bao., Y. (2020) New perspectives on recycling waste glass in manufacturing concrete for sustainable civil infrastructure, *Constr. Build. Mater.*, 257, 119579. https://doi.org/10.1016/j.conbuildmat.2020.119579.

[7] Cyr, M., Idir, R., & Poinot, T. (2012). Properties of inorganic polymer (geopolymer) mortars made of glass cullet, *J. Mater. Sci.*, 47, 2782–2797. https://doi.org/10.1007/ s10853-011-6107-2.

[8] Torres-Carrasco, M., & Puertas, F. (2017). Waste glass as a precursor in alkaline activation: Chemical process and hydration products, *Constr. Build. Mater.*, 139, 342-354. http://dx.doi.org/10.1016/j.conbuildmat.2017.02.071.

[9] AFNOR, NF EN 196-1. (2006). Methods of Testing Cement-Part1: Determination of Strength.

[10] AFNOR, NF EN 196-9. (2010). Methods of Testing Cement. Part 9: Heat of Hydration-Semi Adiabatic Method.

[11] Waples, D. W., & Waples, J. S. (2004). A Review and Evaluation of Specific Heat Capacities of Rocks, Minerals, and Subsurface Fluids. Part 1: Minerals and Nonporous Rocks. *Nat. Resour. Res.*, *13* (2), 97–122. https://doi.org/10.1023/B:NARR.0000032647.41046.e7.

[12] Chase, M. W., Jr. (1998). NIST-JANAF Thermochemical Tables, Fourth Edition. *J Phys Chem Ref Data, Monograph 9*, 1–1951.

[13] Calculated from glass composition and data table available (Pr C. Jacoboni) at: https://ressources.univ-lemans.fr/AccesLibre/UM/Pedago/chimie/03/CHIM310B/chim310B.html

[14] AFNOR, NF EN 12350-2. (2019). Testing fresh concrete – Part 2: slump test.

[15] AFNOR, NF EN 1936. (2007). Natural Stone Test Methods: Determination of Real Density and Apparent Density, and of Total and Open Porosity.

[16] AFNOR, NF P18-459. (2010). Test for Hardened Concrete: Porosity and Density Test.

[17] Johnson, D.R., & Robb, W.A. (1973). Gaylussite: thermal properties by simultaneous thermal analysis. *Am. Mineral.*, 58, 778–784.

[18] Menéndez, E., Andrade, C., & Vega, L. (2012). Study of Dehydration and Rehydration Processes of Portlandite in Mature and Young Cement Pastes. *J. Therm. Anal. Calorim.*, 110 (1), 443–450. https://doi.org/10.1007/s10973-011-2167-4.

[19] Huang, D., Sun, P., Gao, P., Liu, G., Wang, Y., & Chen, X. (2021). Study of the effect and mechanism of alkali-silica reaction expansion in glass concrete. *Sustainability*, 13, 10618. https://doi.org/10.3390/su131910618.

[20] Böttcher, M. E., & Gehlken, P.-L. (1996). Dehydration of Natural Gaylussite and Pirssonite as Illustrated by FTIR Spectroscopy. *N Jb Min. Mh.*, *2*, 73–91.

[21] Gunasekaran, S., Anbalagan, G., & Pandi , S. (2006). Raman and infrared spectra of carbonates of calcite structure, *J. Raman Spactrosc.*, 37, 892-899. https//doi.org/10.1002/jrs.1518.

[22] B. Lafuente, R.T. Downs, H. Yang, N. Stone, The power of databases: the RRUFF project, in: T. Armbruster, R.M. Danisi (Eds.), Highlights in Mineralogical Crystallography, W. De Gruyter, Berlin, Germany, 2015, pp. 1–30. Database accessible from: http://rruff.info/.

[23] Yu, P., Kirkpatrick, R. J., Poe, B., McMillan, P. F., & Cong, X. (1999). Structure of calcium silicate hydrate (C-S-H) : Near-, Mid-, and Far-Infrared Spectroscopy. *J. Am. Ceram. Soc.*, 82, 742-748.